Boson mappings of the fermion dynamical symmetry model

J. Dobeš
Institute of Nuclear Physics, Czech Academy of Sciences, CS 250 68 Řež, Czech Republic

P. Navrátil* and H. B. Geyer
Institute of Theoretical Physics, University of Stellenbosch, Stellenbosch 7600, South Africa
(Received 5 April 1994)

We introduce boson mappings of the fermion dynamical symmetry model (FDSM) to investigate and clarify the relation between the FDSM and the proton-neutron interacting boson model (IBM). The Dyson boson mapping is employed in a dual role–it is first used to obtain exact FDSM results and then as the starting point to obtain some hermitized mappings. By hermitizing the Dyson boson image of the FDSM Hamiltonian through a seniority dictated similarity transformation or by using a Belyaev-Zelevinsky mapping and retaining in both instances one- and two-body terms only, one obtains an IBM type Hamiltonian. FDSM and boson mapped results are then compared for a few typical cases. We reexamine, from the boson point of view, recent statements about an effective SO(6) symmetry when ^{196}Pt is analyzed in the FDSM and about the appearance of normal (maximal F-spin) and exotic states in an application of the FDSM to ^{134}Ba. Throughout our analysis possible spurious states, which may appear as a result of an effective overcompleteness in the (linearly independent) boson basis, are properly identified. We discuss when and where these states appear in the spectra, and the possible implications these considerations may have for allowed representations in the IBM and FDSM.

PACS number(s): 21.60.Ev, 21.60.Cs, 21.60.Fw

I. INTRODUCTION

A shell-model description of collective states in medium-heavy and heavy nuclei remains a formidable task. It is thus almost unavoidable to resort to models in which the link to the original shell-model problem is only tenuous. In the interacting boson model (IBM), [1] boson degrees of freedom are introduced which are believed and, at least in some cases, have been shown, to be related to collective shell-model fermion pairs. The IBM with s and d bosons has proven to be very efficient and useful in phenomenologically describing and correlating extensive pieces of experimental data. Moreover, the IBM, which can be analyzed in terms of an SU(6) group structure, has stimulated considerable activity in the study of collective modes in nuclei from the point of view of dynamical symmetries.

Another model which aims at a description of collective states and relies on algebraic symmetry concepts, is the fermion dynamical symmetry model (FDSM) [2]. In this model, the Ginocchio model [3] is reinterpreted and extended, while the formulation is directly related to the shell structure. The building blocks of the FDSM are namely correlated fermion pairs S, S', and D chosen in a way such that the pair creation and annihilation operators together with a set of multipole operators close an Sp(6) or SO(8) algebra (for S and D) and an SU(2) algebra (for S'). In the FDSM similar symmetry limits as in the IBM are found, though not all of them in a particular valence shell. However, some states of the bosonic IBM are not present in the fermionic FDSM due to the Pauli principle restriction unless a large shell degeneracy is assumed. In this sense the IBM is sometimes regarded as a limit of the FDSM [2], although this seems to be too restrictive an interpretation of the possible relationship.

In the present paper we investigate boson mappings relevant to the fermionic FDSM. This enables us to study some aspects of the relation between the FDSM and IBM rather directly. In doing so, the FDSM situation of no broken pairs and no scattering of pairs between normal and abnormal parity levels (i.e., the proton-neutron Ginocchio model) is considered, but we do not restrict the analysis to dynamical symmetry limits only. We discuss several boson mapping procedures which transcribe an FDSM Hamiltonian into a boson one and compare the results. In this analysis possible spurious states which may appear as a result of an effective overcompleteness in the (linearly independent) boson basis, are properly identified.

Several studies already exist in which the Ginocchio model is bosonized through different boson mappings. Hereby IBM-type Hamiltonians are constructed with an aim to test the applicability of different boson mapping procedures [4,5]. These analyses have been restricted to situations with one kind nucleon only and to a schematic SO(8) Hamiltonian not directly related to any specific nucleus. In the present study, we consider the proton-neutron case and employ Hamiltonians used in actual FDSM calculations [6,7]. The generic Hamiltonian can,

*On leave of absence from the Institute of Nuclear Physics, Czech Academy of Sciences, Řež near Prague, Czech Republic.

e.g., display a transition from vibrational-type spectra to spectra with a rotational character when the number of active nucleons is increased. We mostly focus on the $SO^{\pi}(8)\times Sp^{\nu}(6)$ limit, but in Sec. VI the $SO^{\pi}(8)\times SO^{\nu}(8)$ case is also discussed.

In Sec. II several boson mappings of the Ginocchio model are discussed. In particular, we deal with the Dyson mapping, seniority mapping, and the Belyaev-Zelevinsky mapping. Apart from the possible appearance of spurious states already referred to, the finite Dyson mapping yields exact results. Its nonunitary nature, however, makes a direct comparison with the standard phenomenological IBM difficult. The other two mappings, on the other hand, lead to Hermitian structures for which comparison becomes possible once the associated infinite series expansions have been truncated. In Sec. III the results of the various mapping procedures are compared in different regions of the $Z = 50$–82, $N = 82$–126 shell. ^{196}Pt is analyzed extensively and the concept of an effective SO(6) symmetry in the FDSM [6] is examined. The possible appearance of spurious states in the boson mapped FDSM is addressed in Sec. IV. In Sec. V splitting between normal and exotic states in the $SO(8)\times SO(8)$ FDSM [7] is discussed and conclusions are drawn in Sec. VI.

It should be noted that the correspondence between the IBM and FDSM has also been studied from a group theoretical point of view [8]. Although it is possible to extract some association on the operator level, this analysis differs in spirit from the present mapping analysis and operator association in Ref. [8] is restricted to some multipole operators.

II. BOSON MAPPING OF THE GINOCCHIO MODEL

In the Ginocchio model creation and annihilation operators of S and D fermion pairs are introduced which, together with some multipole operators P, close an algebra. According to whether either the pseudo-orbital angular momentum $k = 1$ or pseudospin $i = 3/2$ is treated as active [2,3], an Sp(6) or SO(8) algebra is, respectively, realized. (See Ref. [2] for definitions and terminology adopted.) The fermion Hamiltonian is written in terms of the pair and multipole operators and should generally be diagonalized in the fermion space constructed by successive action of the pair creation operators onto the fermion vacuum, as, e.g., implemented in the FDSM computer code FDUO [9].

A. Dyson mapping

When a fermion Hamiltonian is expressed in terms of the generators of a given algebra, as in the case of the Ginocchio or FDSM models, one may obtain an equivalent boson Hamiltonian from the generalized Dyson boson mapping (DBM) in a straightforward way. For the Sp(6) and SO(8) algebras, the Dyson boson realization is written in terms of s and d boson operators, as appears, e.g., in Refs. [10,11]. In particular, the monopole pair operators and the quadrupole, dipole, and octupole operators of the FDSM map as follows:

$$S^{\dagger} \to \sqrt{\Omega}\Big(s^{\dagger} - \frac{1}{\Omega}s^{\dagger}s^{\dagger}s - \frac{2}{\Omega}s^{\dagger}d^{\dagger}\cdot\tilde{d} - \frac{1}{\Omega}d^{\dagger}\cdot d^{\dagger}s - \frac{1}{\Omega}\chi(d^{\dagger}d^{\dagger})^{(2)}\cdot\tilde{d}\Big), \tag{2.1}$$

$$S \to \sqrt{\Omega}s, \tag{2.2}$$

$$P^2 \to (d^{\dagger}s + s^{\dagger}\tilde{d})^{(2)} + \chi(d^{\dagger}\tilde{d})^{(2)}, \tag{2.3}$$

$$P^1 \to \sqrt{2}(d^{\dagger}\tilde{d})^{(1)}\ ,\ P^3 \to -\sqrt{2}(d^{\dagger}\tilde{d})^{(3)}\ \ [\mathrm{SO}(8)\,\mathrm{case}], \tag{2.4}$$

$$P^1 \to \tfrac{1}{2}\sqrt{15}(d^{\dagger}\tilde{d})^{(1)}\ \ [\mathrm{Sp}(6)\,\mathrm{case}]. \tag{2.5}$$

The pair degeneracy of the fermion space is denoted by Ω, while $\chi = \sqrt{7}/2$ or 0 for the Sp(6) and SO(8) algebras, respectively.

When the mapped Dyson Hamiltonian is to be diagonalized a proper basis has to be chosen. The boson mapping formalism is constructed to yield results identical to those obtained in the fermion space if the physical basis is used, namely, the set of boson states obtained by simultaneously replacing in any fermion basis state each generator by its boson image and switching from the fermion to boson vacuum. Not only is this a cumbersome operation, but it may also obscure the relationship to boson phenomenology where the natural ideal boson basis is used. This basis is constructed by successive action of the *boson* creation operators (not the mapped generators) onto the boson vacuum and it is well known that the eigenvalues and eigenstates emerging from this choice will include those obtained by diagonalization of the fermion Hamiltonian or, equivalently, diagonalization of the mapped boson Hamiltonian in the physical basis.

For the number of fermion pairs $N > \Omega/3$ [Sp(6)] or $N > \Omega/2$ [SO(8)], the dimension of the ideal boson basis is, however, larger than the original fermion space, due to the presence of states which correspond to Pauli forbidden fermion states. Unphysical (spurious) solutions of the boson Hamiltonian then appear together with the exact physical ones. They are, however, separated from the physical solutions [12] and methods exist which allow their identification [12,13].

We discuss the role of possible spurious solutions in more detail in Sec. IV. Here we only note that the Dyson Hamiltonian has a two-body structure, though it generally is non-Hermitian. The existing computing machinery of the IBM, as, e.g., in Ref. [14] could thus be adopted easily to develop an alternative FDSM computer program. Some earlier calculations in Ref. [15] are carried out similarly, although spurious states need not be considered there. Recent calculations for SO(12) and Sp(10) models have likewise capitalized on the simpler calculational options in the boson space [16]. In fact, this boson space approach has often been used for exact

calculations in SO(5)-type fermion models where one additionally profits from the fact that only three types of scalar bosons appear [12,17,18].

The non-Hermiticity of the Dyson boson Hamiltonian makes it different from the traditional Hamiltonian of the IBM. To obtain a Hermitian Hamiltonian, equivalent to the Dyson one at least in the physical sector, a similarity transformation naturally comes to mind. Two practical procedures are considered for its construction. In the first, referred to as the seniority mapping, the SU(2) aspects of the original algebras of the Ginocchio model are stressed. The second procedure, called the Belyaev-Zelevinsky (BZ) mapping hereafter, aims at an exact treatment of the SU(3) and SO(6) chains of the Sp(6) and SO(8) algebras, respectively.

B. Seniority mapping

The seniority mapping starts from the observation that in the Dyson mapped boson ket states there is no straightforward relation between the seniority v of fermion states and the number of non-s bosons (equivalently d bosons here). The Dyson image of the $v = 0$ state $(S^\dagger)^N|0\rangle$ in fact contains components with two or more d bosons. In contrast one aims in the seniority mapping to establish simple relations between fermion states with good seniority and boson states with a fixed number of d bosons, such as

$$|N, v = 0\rangle \leftrightarrow |n_s = N), \tag{2.6}$$

$$|N, v = 2\rangle \leftrightarrow |n_s = N - 1, n_d = 1). \tag{2.7}$$

To achieve this, one could impose the conditions that the seniority images of the $S^\dagger$ and S operators are given by the Dyson mapping

$$S^\dagger \to \sqrt{\Omega}\Big(s^\dagger - \frac{1}{\Omega}s^\dagger s^\dagger s - \frac{2}{\Omega}s^\dagger d^\dagger \cdot \tilde{d}\Big), \tag{2.8}$$

$$S \to \sqrt{\Omega}s \tag{2.9}$$

of the SU(2) subalgebra, rather than Eq. (2.1). It is simple to see that the above mapping is still a proper realization of SU(2) and that it provides us with a Hermitian image of the fermion pairing Hamiltonian $S^\dagger S$. One could then continue to find the images of other operators by, e.g., inspecting the commutation relations. In principle this construction has many solutions. One of them is found by noticing that the images of the pairing Hamiltonian resulting from the mappings (2.1) and (2.8), respectively, are related by a similarity transformation [19]. This transformation then enables one to construct the seniority images of the fermion operators from their original Dyson forms. Although a closed form of the similarity transformation exists for the SO(8) case, it is generally only known in infinite series form [19]. In actual construction, only the lowest-order terms are used to find seniority images of the non-SU(2) generators. For the quadrupole operator this yields (the relevant techniques are discussed in Refs. [19–21])

$$P^2_{\rm sen} = s^\dagger\tilde{d} + \Big(1 - \frac{n_s}{\Omega + 1 - 2N + 2n_s}\Big)d^\dagger s + \chi\Big(1 - \frac{2n_s}{\Omega - 2N + 2n_s}\Big)(d^\dagger\tilde{d})^{(2)}. \tag{2.10}$$

The images of the dipole and octupole operators P^1 and P^3 are invariant under the similarity transformation, as follows from arguments about angular momentum and boson seniority conservation in the similarity transformation. The seniority image for the D pair operator is discussed in Refs. [19,22]. Here, we do not consider it further, as in the FDSM Hamiltonian the quadrupole pairing term can be replaced by redefining the other parameters [2].

In expression (2.10) for the seniority quadrupole operator two-body terms which contain the number operator n_s for s bosons in a coefficient are retained. The total number of fermion pairs (or total number of bosons) is denoted as N, a fixed number for a given configuration. To approximate this structure as a one-body operator, we employ two procedures. In the first, denoted in the following as the seniority mapping A, the operator n_s is substituted by its value in a seniority $v = 2$ state, i.e., by $N - 1$. In actual FDSM calculations, the low-lying states could, however, be quite different from the seniority classification scheme. To take this into account more accurately, we use alternatively a seniority mapping B in which n_s is replaced by $N - 1 - \frac{1}{2}\langle v\rangle$, where $\langle v\rangle$ is the mean value of the seniority in the FDSM ground state. This mean value is calculated from the relation

$$\langle S^\dagger S\rangle = \tfrac{1}{4}(2N - \langle v\rangle)(2\Omega - 2N - \langle v\rangle + 2). \tag{2.11}$$

With either of these approximations the seniority image of the quadrupole operator becomes a one-body operator, although it is still not self-conjugate. To Hermitize it, we apply the Hermitization procedure of Refs. [23,19,21] to obtain the respective seniority images of the quadrupole operator as

$$P^2_{\rm senA} = \sqrt{1 - \frac{N-1}{\Omega - 1}}(d^\dagger s + s^\dagger\tilde{d})^{(2)} + \chi\Big(1 - \frac{2N-2}{\Omega - 2}\Big)(d^\dagger\tilde{d})^{(2)}, \tag{2.12}$$

$$P^2_{\rm senB} = \sqrt{1 - \frac{N - \frac{1}{2}\langle v\rangle - 1}{\Omega - 1 - \langle v\rangle}}(d^\dagger s + s^\dagger\tilde{d})^{(2)} + \chi\Big(1 - \frac{2N - \langle v\rangle - 2}{\Omega - \langle v\rangle - 2}\Big)(d^\dagger\tilde{d})^{(2)}. \tag{2.13}$$

The mapping A in expression (2.12) is the same as obtained in the Otsuka-Arima-Iachello (OAI) procedure [24] discussed in Ref. [4], whereas the mapping B (2.13) is more in the spirit of the OAI-Talmi (OAIT) approach [25].

C. Belyaev-Zelevinsky mapping

In the BZ method, the boson images of the multipole operators are the same as in the Dyson mapping. The images of the pair operators are constructed to obey the commutation relations of the algebra and to conserve the self-conjugacy of the fermion operators. This generally leads to infinite series for the images of the pair operators which may, however, be expressed in a closed form in terms of Casimir operators or their eigenvalues. For the SO(8) model such a mapping was given in Ref. [4] and for the Sp(6) model, in a slightly modified version, in Ref. [26]. As we want to construct an IBM-like Hamiltonian with one- and two-body terms only, we retain in the images of the S-pair operators only those terms which can contribute to such a Hamiltonian. For SO(8) this means the approximation

$$S^\dagger \to s^\dagger\sqrt{\Omega-2N} + \tfrac{1}{2}(s^\dagger s^\dagger - d^\dagger\cdot d^\dagger)s\frac{\sqrt{\Omega+4}-\sqrt{\Omega-2N}}{N+2} \tag{2.14}$$

and its conjugate. It gives exact matrix elements between the lowest SO(6) states $|N,\sigma=N\rangle$ and $|N+1,\sigma=N\pm1\rangle$. For the Sp(6) case we similarly have

$$S^\dagger \to s^\dagger\sqrt{\Omega-3N} - \left[d^\dagger\cdot d^\dagger s - s^\dagger n_d - 2s^\dagger s^\dagger s + \tfrac{\sqrt{7}}{2}d^\dagger\cdot(d^\dagger\tilde{d})^{(2)}\right]\frac{\sqrt{\Omega+\frac{3}{2}}-\sqrt{\Omega-3N}}{3N+\frac{3}{2}}, \tag{2.15}$$

which reproduces the matrix elements between the lowest SU(3) states $|N,(\lambda=2N,\mu=0)\rangle$ and $|N+1,(\lambda=2N+2,\mu=0)\rangle$, $|N+1,(\lambda=2N-2,\mu=2)\rangle$.

The IBM-like boson image of the pairing interaction is then obtained by combining either of the above expressions with its conjugate and retaining the one- and two- body terms only. To make contact with the FDSM or IBM, an explicit N dependence of the strength parameters must then still be eliminated. To achieve this the N dependence in the first terms of the images of $S^\dagger$ and S is retained in their mutual product, whereas in all the other products we set N=2. This ensures that we recover the (correct) first three terms of the DBM image (2.1) with coefficients modified but independent of N, together with some additional two-body terms which also have coefficients independent of N. The resulting Hermitian Hamiltonian is exact for total boson number $N=1$ and $N=2$.

Both the seniority mapping and the BZ mapping can thus be approximated to map the FDSM Hamiltonian into a Hermitian Hamiltonian of the IBM type with one- and two-body terms only. In the seniority mapping B, we use some knowledge of the FDSM solution via $\langle v\rangle$ [see Eqs. (2.11) and (2.13)]. In principle an iteration procedure might also be used to find a value for $\langle n_s\rangle$ solely in the boson approach. One could start with seniority mapping A calculations and substitute in subsequent iterative steps $\langle n_s\rangle$ by $N-1-\langle n_d\rangle$, where $\langle n_d\rangle$ is obtained from the 0_1^+ state of the previous step.

III. COMPARISON OF FDSM AND MAPPED BOSON APPROACH

In the present section we compare results of the FDSM with those obtained by the boson mapping procedures described above. Examples from the Z=50–82, N=82–126 shell are discussed for which the coupled $\mathrm{Sp}^\nu(6)\times\mathrm{SO}^\pi(8)$ symmetry in the FDSM is indicated.

As is common in the FDSM, we assume that a description with no broken pairs and no scattering of pairs between the normal and abnormal parity levels is appropriate for low-lying levels. The corresponding general one- and two-body FDSM Hamiltonian then contains 11 parameters. A further reduction of parameters has been employed (see Refs. [2,6]) in the simplified Hamiltonian

$$H = G_{0\pi}S_\pi^\dagger S_\pi + G_{0\nu}S_\nu^\dagger S_\nu + B_{2\pi}P_\pi^2\cdot P_\pi^2 + B_{2\nu}P_\nu^2\cdot P_\nu^2 + B_{2\pi\nu}P_\pi^2\cdot P_\nu^2 . \tag{3.1}$$

where now only five parameters appear. In the FDSM the number N_1 of pairs in the normal parity level are expressed in terms of the total number N of nucleon pairs by the semiempirical formula $N_1=0.75+0.5N$, except that $N_1=N-\Omega_0$ if the abnormal parity level with the pair degeneracy Ω_0 is completely filled ($N>2\Omega_0+1.5$) [2].

The electromagnetic quadrupole operator is taken in the one-body form

$$T(E2) = e_\pi P_\pi^2 + e_\nu P_\nu^2 . \tag{3.2}$$

We now employ the Hermitian boson mappings above to map the fermion Hamiltonian (3.1) and operator $T(E2)$ onto a one- plus two-body boson Hamiltonian and a one-body boson quadrupole operator of the IBM-2 type. Results from the ensuing diagonalization are compared with exact FDSM results, obtained by employing the Dyson boson images.

A. ^{196}Pt nucleus

Within the IBM context, the ^{196}Pt nucleus is considered to be a fine example of the O(6) dynamical symmetry limit. In the $\mathrm{Sp}^\nu(6)\times\mathrm{SO}^\pi(8)$ FDSM, no coupled neutron-proton O(6) symmetry exists, however. Nevertheless, it was recently claimed in Ref. [6] that the FDSM describes the ^{196}Pt spectra and $E2$ transitions accurately

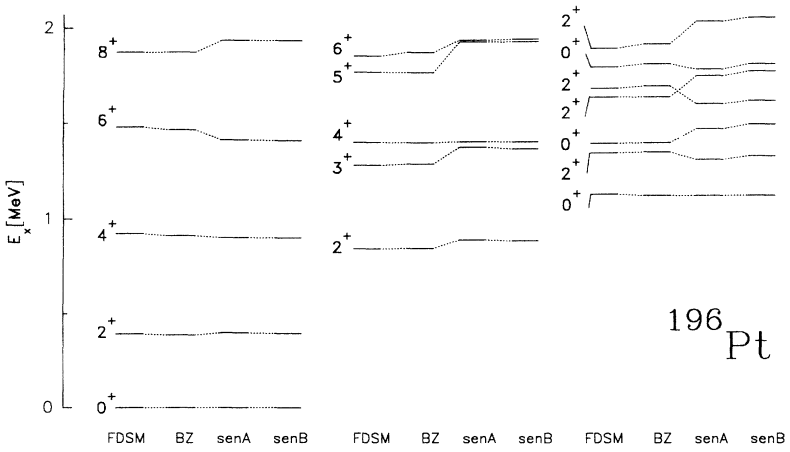

FIG. 1. Calculated excitation energies for ^{196}Pt. Results from the FDSM and mapped boson approaches are compared.

and that one can thus argue for the existence of an effective SO(6) symmetry in the FDSM.

In Fig. 1, the calculated energy levels as obtained by the FDSM (via Dyson mapping) and the Hermitian boson mappings are displayed. The FDSM parameters of Ref. [6] are used wherein also experimental and FDSM excitation energies are compared. The $B(E2)$ values are given in Table I and some $B(E2)$ branching ratios are found in Table I. The absolute value of the effective fermion $E2$ charge is fixed by matching the FDSM value to the experimental $B(E2, 2_1^+ \rightarrow 0_1^+)$ strengths. Note that for ^{196}Pt the counting rule for the number of pairs in the FDSM agrees with that of the boson number for IBM-2. All the boson mappings investigated give results very similar to those of the FDSM, with the BZ mapping being quantitatively most precise. The seniority mappings fail for some of the higher-lying states.

As compared to experiment and also to the IBM calculations [28,29], the FDSM $B(E2)$ values for the ground-state band cut off too rapidly with increasing spin. Inclusion of Coriolis antipairing in a more complete scheme could possibly remedy this defect. Then the calculated energy of the 8_1^+ would, however, decrease and in the particular case of ^{196}Pt the difference between the FDSM (1.876 MeV) and experimental (2.253 MeV) excitation energies of the 8_1^+ state would in fact be enhanced.

The FDSM results for $E2$ transitions from some of the higher-lying states are also not satisfactory. In the IBM O(6) classification scheme these states are associated with the O(6) representation $\sigma = N - 2$, which differs from the representation $\sigma = N$ relevant to the ground-state band. Actually, transitions from these states are considered to be an appropriate test for the realization of an SO(6) symmetry [30]. For example, the $0_3^+ \rightarrow 2_2^+$ transition is forbidden in O(6) by both the O(6) (σ) and SO(5) (τ) selection rules and it is in fact very weak experimentally. In contrast, the FDSM predicted $B(E2)$ value for this transition is comparable with values for inter-band allowed transitions (cf. Table I). The $E2$ branching ratios from the 2_4^+ state, found in Table II, are also not correctly given by the FDSM.

The above deficiency suggests that when $E2$ transi-

TABLE I. The $E2$ properties for ^{196}Pt. The $E2$ experimental values are from Refs. [27,28]. $B(E2)$ probabilities are given in units of e^2b^2.

$B(E2)$	Expt.	FDSM	BZ	sen A	sen B
$2_1^+ \rightarrow 0_1^+$	0.3	0.300	0.302	0.280	0.295
$4_1^+ \rightarrow 2_1^+$	0.443	0.397	0.403	0.379	0.398
$6_1^+ \rightarrow 4_1^+$	0.494	0.355	0.372	0.383	0.400
$8_1^+ \rightarrow 6_1^+$	0.577	0.265	0.269	0.332	0.344
$2_2^+ \rightarrow 0_1^+$	2×10^{-6}	0.0004	0.0010	0.0003	0.0005
$2_2^+ \rightarrow 2_1^+$	0.262	0.415	0.403	0.357	0.367
$4_2^+ \rightarrow 2_1^+$	0.0023	0.0036	0.0040	0.0025	0.0034
$4_2^+ \rightarrow 2_2^+$	0.218	0.189	0.191	0.189	0.195
$4_2^+ \rightarrow 4_1^+$	0.218	0.202	0.200	0.168	0.170
$6_2^+ \rightarrow 4_1^+$	0.0037	0.0485	0.0405	0.0225	0.0258
$6_2^+ \rightarrow 4_2^+$	0.350	0.136	0.139	0.229	0.239
$6_2^+ \rightarrow 6_1^+$	0.085	0.106	0.105	0.0816	0.079
$8_2^+ \rightarrow 6_2^+$	0.375	0.170	0.170	0.177	0.188
$0_2^+ \rightarrow 2_1^+$	0.033	0.122	0.128	0.116	0.118
$0_2^+ \rightarrow 2_2^+$	0.142	0.277	0.310	0.213	0.266
$2_3^+ \rightarrow 2_1^+$	0.0009	0.0003	0.0003	0.00007	0.0009
$0_3^+ \rightarrow 2_1^+$	<0.034	0.0068	0.0081	0.0038	0.0049
$0_3^+ \rightarrow 2_2^+$	<0.002	0.228	0.206	0.232	0.207

TABLE II. $E2$ branching ratios from the level 2_4^+ of ^{196}Pt.

	Expt.	FDSM	BZ	sen A	sen B
$2_4^+ \to 0_1^+$	0.01	0.012	0.077	0.035	0.026
2_1^+	0.3	0.32	0.209	18.4	14.1
2_2^+	0.5	0.0008	0.069	6.72	1.75
4_1^+	1.7	5.64	6.88	15.44	5.33
3_1^+	0.4	384.0	417.0	1198.0	931.0
0_2^+	<0.3	55.7	71.3	154.5	87.2
4_2^+	<3.0	27.3	25.7	31.5	17.6
2_3^+	<15.0	105.1	109.3	559.3	420.2
0_3^+	100.0	100.0	100.0	100.0	100.0

tions are also considered, no effective fermion SO(6) dynamical symmetry emerges in the FDSM calculations of Ref. [6]. One could perhaps rather speak about a fermion SO(5) symmetry which determines transitions within a particular SO(6) representation. No coupled neutron-proton SO(5) symmetry exists in the $\mathrm{Sp}^\nu(6)\times\mathrm{SO}^\pi(8)$ FDSM either, and the suggested SO(5) FDSM symmetry should again be understood as an effective one.

In Table III we show overlaps of the boson wave functions obtained from the mapped Hamiltonians with the corresponding $\mathrm{SO}^{\pi+\nu}(6)$ wave functions. The FDSM column in this table has been calculated from the Dyson mapping. The small overlaps again confirm the conclusions of the preceding paragraph. The maximal F-spin content of the individual states is also shown. We observe that F spin is not a good quantum number for the low-lying states at all, which also suggests that the IBM SO(6) symmetry is absent in the present Hamiltonian.

B. Deformed nuclei

Using the set of the FDSM parameters from the ^{196}Pt analysis, a transition to the rotational regime is obtained by changing only the number of valence pairs [6]. As an illustration, we discuss calculations with the number of FDSM pairs in the natural parity orbits being $N_\nu = 4$ and $N_\pi = 4$. These numbers correspond to the deformed isotopes ^{158,160}Gd. As we only aim in this subsection at a qualitative discussion of the FDSM and applicability of its boson mapped versions, we do not perform a final tuning of parameters with respect to experiment and simply use the ^{196}Pt set.

In Fig. 2 the spectra given by the FDSM and boson mapped Hamiltonians are compared. In Table IV, the calculated $B(E2)$ values are displayed. The seniority mapping procedures give results differing appreciably from the exact FDSM results. This should be expected as the seniority mapping is tailored mainly to the vibrational SU(2) regime with prevailing importance of the pairing components in the Hamiltonian. The BZ mapping treats the multipole-multipole part of the Hamiltonian exactly, which is crucial for the rotational character of spectra. Indeed, the BZ mapped results agree reasonably well with the FDSM calculations.

C. Vibrational nuclei

As an example of a vibrational nucleus, we consider $N_\nu = 2$ and $N_\pi = 4$. The semiempirical FDSM counting rule for active pairs indicates that these numbers correspond to the ^{148}Sm nucleus. The set of the FDSM parameters used in the ^{196}Pt analysis does not yield vibrational-type spectra. However, by slightly modifying the pairing strengths to $G_{0\nu} = G_{0\pi} = -97$ keV and retaining the quadrupole-quadrupole strengths of Ref. [6], one reproduces the experimental spectrum of ^{148}Sm reasonably well. Again, we do not attempt a parameter search for a best fit to the experimental data.

In Fig. 3 the calculated and experimental spectra are shown. The $B(E2)$ strengths are given in Table V. Results of the seniority mapping procedures A and B are very close so that only for the former one are displayed. As expected, seniority mapping procedures agree reasonably well with the FDSM results. The BZ mapping even more closely reproduces the FDSM calculations. Though the BZ mapping introduced in Sec. II does not reflect the pairing part of the FDSM Hamiltonian in all detail, it is still exact up to two pairs and sufficiently precise for small numbers of pairs such as 3 or 4. These numbers are just those relevant for vibrational nuclei.

TABLE III. Overlaps of the $\mathrm{SO}^{\pi+\nu}(6)$ wave functions with the wave functions of different boson mapped Hamiltonians as well as their maximal F-spin content is shown. FDSM results are obtained using the Dyson boson mapping.

	FDSM		BZ		sen A		sen B	
	$\mathrm{SO}^{\pi\nu}(6)$ overlap	max F spin	$\mathrm{SO}^{\pi\nu}(6)$ overlap	max F spin	$\mathrm{SO}^{\pi\nu}(6)$ overlap	max F spin	$\mathrm{SO}^{\pi\nu}(6)$ overlap	max F spin
0_1^+	0.37	0.68	0.37	0.68	0.54	0.80	0.56	0.80
0_2^+	0.04	0.66	0.08	0.66	0.15	0.82	0.17	0.82
2_1^+	0.46	0.70	0.45	0.70	0.64	0.82	0.65	0.82
2_2^+	0.58	0.70	0.56	0.70	0.75	0.82	0.76	0.83
4_1^+	0.59	0.72	0.56	0.72	0.75	0.84	0.76	0.84
4_2^+	0.59	0.64	0.54	0.62	0.68	0.75	0.68	0.76
6_1^+	0.63	0.67	0.59	0.67	0.71	0.78	0.70	0.78
8_1^+	0.28	0.43	0.28	0.44	0.51	0.61	0.52	0.62

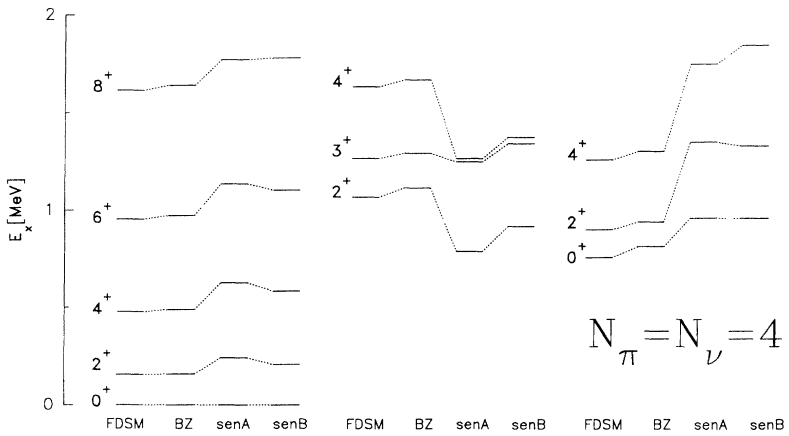

FIG. 2. Calculated excitation energies for the case of a deformed nucleus with $N_\nu = N_\pi = 4$. Results from the FDSM and mapped boson approaches are compared.

IV. SPURIOUS STATES IN BOSON SPACE

For the numbers of pairs $N_\nu > \Omega_\nu/3 = 5$ (82–126 shell) and $N_\pi > \Omega_\pi/2 = 5$ (50–82 shell), spurious states occur in the boson space when the ideal boson basis is used [13]. Although the ideal boson basis states themselves are linearly independent, they correspond for the pair numbers above to fermion states which are linearly dependent. After diagonalization they thus give rise to states which have no correspondent states in the original FDSM space. In terms of the single-fermion labels, the Pauli principle is violated in these states. For the proton SO(8) part, the problem of spurious states is circumvented by resorting to fermion particle-hole symmetry and counting fermion hole pairs from the end of the shell. This leads to a precise one-to-one correspondence between fermion pair states and ideal boson basis states [3]. For the neutron Sp(6) part, this loophole does not save the day and spurious states would still appear. In the FDSM scheme of counting pairs in normal parity levels, such a situation occurs for $N_\nu = 6$ or 7 in the 82–126 shell.

TABLE IV. Reduced $B(E2)$ matrix elements (in arbitrary units) for $N_\pi = N_\nu = 4$ calculations. The same Hamiltonian parameters as for the ^{196}Pt are used.

	FDSM	BZ	sen A	sen B
2^+(g.s.) $\rightarrow$ 0^+(g.s.)	9.8	9.8	8.0	8.8
4^+(g.s.) $\rightarrow$ 2^+(g.s.)	15.6	15.6	12.8	14.1
6^+(g.s.) $\rightarrow$ 4^+(g.s.)	19.0	19.0	15.9	17.3
8^+(g.s.) $\rightarrow$ 6^+(g.s.)	20.6	20.6	17.8	19.2
2^+(g.s.) $\rightarrow$ 2^+(g.s.)	11.7	11.6	7.5	9.8
4^+(g.s.) $\rightarrow$ 4^+(g.s.)	15.2	15.1	9.3	12.3
6^+(g.s.) $\rightarrow$ 6^+(g.s.)	18.7	18.6	10.8	14.6
8^+(g.s.) $\rightarrow$ 8^+(g.s.)	21.8	21.7	11.9	16.5
$3^+(\gamma) \rightarrow 2^+(\gamma)$	11.2	10.6	9.0	9.2
$4^+(\gamma) \rightarrow 2^+(\gamma)$	8.6	8.6	9.2	9.9
$2^+(\gamma) \rightarrow 2^+(\gamma)$	4.9	6.3	- 6.3	- 7.8
$2^+(\beta) \rightarrow 0^+(\beta)$	7.7	7.3	5.3	5.8
$4^+(\beta) \rightarrow 2^+(\beta)$	12.4	11.9	7.6	8.4
$2^+(\beta) \rightarrow 2^+(\beta)$	- 4.2	- 5.6	6.3	7.8
$2^+(\gamma) \rightarrow 0^+$(g.s.)	-1.3	- 1.3	- 1.5	- 1.7
$3^+(\gamma) \rightarrow 2^+$(g.s.)	2.6	2.7	2.2	2.6
$2^+(\gamma) \rightarrow 2^+$(g.s.)	1.0	0.7	6.2	4.8
$2^+(\beta) \rightarrow 0^+$(g.s.)	1.2	1.3	0.5	0.7
$2^+(\beta) \rightarrow 2^+$(g.s.)	- 3.3	- 3.5	- 0.02	- 0.1
$2^+(\gamma) \rightarrow 2^+(\beta)$	9.0	8.1	1.9	3.1
$3^+(\gamma) \rightarrow 2^+(\beta)$	- 6.1	- 7.1	- 4.9	- 6.8
$2^+(\gamma) \rightarrow 0^+(\beta)$	4.2	4.8	4.0	4.9

In principle, one could select the physical part of the boson space by using the SU(6)$\supset$SU(3) classification scheme for the construction of the neutron boson basis and disregarding the Pauli forbidden SU(3) (λ,μ) representations (12,0) for $N_\nu = 6$ and (14,0) and (10,2) for $N_\nu = 7$. Alternatively, we use the SU(6)$\supset$SU(5) classification of the boson basis in which physical and spurious components do mix. Hamiltonian diagonalization, however, separates physical and unphysical eigenstates and we determine the respective character of an eigenstate by the method of Ref. [12]. According to this analysis one exploits the structure

$$(\tilde{\varphi}_{\rm spur}|\Theta_D|\psi_{\rm phys}) = 0\,, \tag{4.1}$$

$$(\tilde{\psi}_{\rm phys}|\Theta_D|\varphi_{\rm spur}) \neq 0\,. \tag{4.2}$$

where Θ_D is the Dyson boson image of any fermion test operator Θ other than the Hamiltonian. Testing matrix elements with an arbitrary combination of the proton and neutron angular momentum operators P^1, one identifies the unphysical solutions easily. Of course, exact separation works only for the exact boson mapping, namely, for the Dyson mapping in our treatment. In the case of approximate mappings, as the seniority and BZ mappings above are, the physical and unphysical components would be mixed in Hamiltonian eigenstates and identification then becomes more elaborate [31].

With the most symmetric $(2N,0)$ SU(3) representation forbidden, together with whichever other representations are also implied, it seems that an unpleasant consequence emerges which led Ginocchio to disregard the Sp(6) fermion algebra in his seminal paper [3]. Namely, the forbidden representations, when viewed from and included in the IBM SU(6)$\supset$SU(3) limit, are related to the

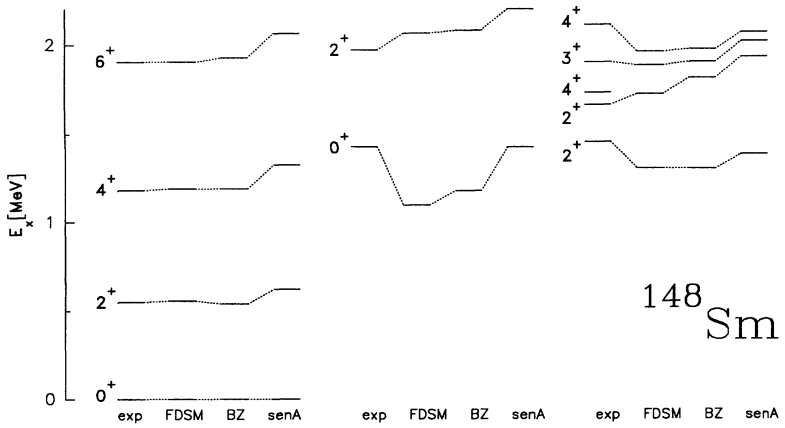

FIG. 3. Calculated excitation energies for ^{148}Sm. Experimental results and results calculated from the FDSM and mapped boson approaches are compared.

lowest-lying bands in deformed nuclei and are experimentally well established. Without them one would have difficulty in the description of experimental spectra. In the FDSM, this dilemma is partly alleviated by considering only pairs in normal parity levels. This counting excludes fewer nuclei for which forbidden representations occur. Nevertheless, some species of deformed nuclei in the rare earth region would still need neutron pair numbers of $N_\nu = 6$ or 7 in an FDSM description, so that the problem is not completely resolved.

In the FDSM studies [2] arguments have been collected to the effect that the elimination of the forbidden representations has favorable consequences for the description of $B(E2)$ systematics and ground-state binding energies. Unless it is possible to address spectra successfully from the same point of view, some doubt about the situation remains. So far the corresponding nuclei have not been analyzed within the FDSM.

In Fig. 4 FDSM results are shown for the pair numbers $N_\nu = 7$ and $N_\pi = 4$. According to the FDSM counting rule, these numbers are appropriate for the $^{176-182}$Yb or $^{178-184}$Hf nuclei. These nuclei are intermediate between the Gd and Pt isotopes discussed in the previous section. For our purposes we therefore simply again adopt the FDSM parameters from the ^{196}Pt analysis.

It is clear that the calculated FDSM spectrum does not resemble the experimental one. The too small calculated moment of inertia may be improved perhaps by a parameter variation and certainly by an inclusion of the $P^1 \cdot P^1$ term. The main deficiency of the FDSM results appears to be in low-lying calculated $K = 2^+, 0^+$, and 4^+ bands. This is a reflection of the fact that for $N_\nu = 7$ in the SU(3) limit, the lowest-lying physical representation (6,4) contains degenerate $K = 0^+, 2^+$, and 4^+ bands. Departing from the SU(3) limit, as well as including the proton configuration, removes the degeneracy, but does not prevent these three bands from still lying close together. Note for example, that after subtraction of the rotational contribution, the first excited band becomes the $K = 4^+$ band which is only about 0.3 MeV above the ground-state band.

In Fig. 4 unphysical states which result from diagonalization of the Dyson mapped Hamiltonian are not shown. Their positions are spread around the middle of the physical states. Some of the unphysical eigenvalues of the non-Hermitian Dyson Hamiltonian are complex conjugate pairs. The lowest Dyson Hamiltonian eigenvalue corresponds to a physical state. This can be linked to the repulsive quadrupole-quadrupole interaction between like fermions in the Hamiltonian. When these repulsive contributions are removed, the energies of the spurious states shift down below the physical ones. This is in accordance with our previous model calculations [22,32] where it was found that for an attractive quadrupole-quadrupole interaction, the lowest-lying states of the Dyson mapped Hamiltonian are unphysical.

It has been conjectured that inclusion of the pair scattering between normal and abnormal parity levels might be important for a description of nuclei for which forbidden SU(3) representations occur [2]. Indeed, the pair scattering could effectively decrease the number of active pairs and remedy some of the unpleasant features described above. One might then wonder whether such a mechanism would not act differently for nuclei with neutrons considered as particles or holes and what the modification will be to the FDSM semiempirical formula for the numbers of pairs in the normal parity levels (see Sec. III). In any case, the FDSM analysis of nuclear spectra in regions with eliminated forbidden representations remains to be carried out.

TABLE V. B(E2) probabilities for the ^{148}Sm in units of e^2b^2. Effective nucleon charges $e_\pi = e_\nu$ are chosen to normalize the FDSM value to the $2_1^+ \to 0_1^+$ experimental value.

B(E2)	Expt.	FDSM	BZ	sen A
$2_1^+ \to 0_1^+$	0.151(10)	0.151	0.156	0.135
$4_1^+ \to 2_1^+$	0.25(7)	0.249	0.250	0.201
$2_2^+ \to 0_1^+$	0.0069(11)	0.0039	0.0034	0.0014

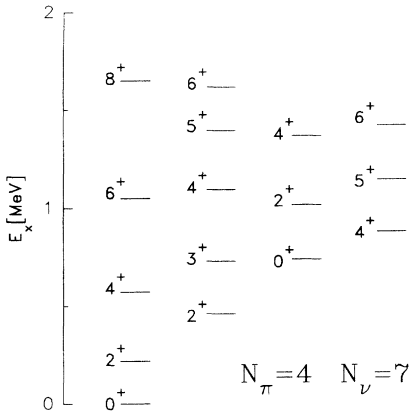

FIG. 4. FDSM calculated excitation energies for the case with $N_\nu = 7$ and $N_\pi = 4$. These numbers should correspond to a deformed nucleus in the A=180 region. Unphysical states appear in the Dyson boson mapped version of the FDSM. These are not shown in the figure.

V. SO$^\pi$(8)×SO$^\nu$(8) MODEL: NORMAL AND EXOTIC STATES

In the proton-neutron version of the IBM (IBM-2), a so-called F-spin operator is introduced to address a possible proton-neutron boson symmetry [33]. The F-spin number is connected with the classification of the U$^{(\pi+\nu)}$(6) subgroup of the IBM-2 space. It is observed that states of maximal F spin (maximal proton-neutron symmetry) lie in the lower part of the spectra, while states with lower F-spin values (mixed symmetry states) have been identified at higher excitation energies.

Since the U$^{(\pi+\nu)}$(6) subgroup does not appear in the FDSM, it is not possible to define the corresponding F-spin operator there. Nevertheless, it has recently been argued that in the FDSM the proton-neutron symmetry can be followed and that the splitting between normal (maximal F-spin) states and exotic (lower F-spin) states emerges naturally [7]. The spectrum and electromagnetic properties of ^{134}Ba were examined in detail. It was also argued in Ref. [7] that there are different mechanisms responsible for the splitting in the IBM-2 and in the FDSM—the Majorana interaction pushes up the mixed symmetry states in the IBM-2, whereas the proton-neutron interaction causes the splitting of normal and exotic states in the FDSM.

In this section, we repeat the ^{134}Ba calculation of Ref. [7] using the boson mapped versions of the FDSM. Working within the boson space enables us to evaluate the maximal F-spin content of individual states. Note that the bosonic F-spin operator is not an image of any FDSM operator. The boson mapping procedure, however, gives us a mechanism to quantify the notion of FDSM proton-neutron symmetry.

The FDSM Hamiltonian used for ^{134}Ba calculations is taken from Ref. [7]. It is given by Eq. (3.1) with the quadrupole-quadrupole interaction between like nucleons omitted. To improve the fit, the octupole-octupole proton-neutron interaction $\lambda P_\pi^3 \cdot P_\nu^3$ is added. In Table VI, we present results of exact FDSM (DBM) calculations and the BZ approximation. Note that $N_\pi = 3$ and $N_\nu = 2$ for ^{134}Ba, which means that the BZ mapping treats the neutron part exactly. Consequently, the IBM-2 calculations with the BZ Hamiltonian are expected to approximate the FDSM ones very well. This is confirmed in Table VI where energies of some low-lying states and their maximal F-spin content are given. We observe that the normal states indeed have a high degree of F-spin purity. The 2_3^+ state is an exotic state, in accordance with the conclusions of in Ref. [7]. In Table VI seniority mapping A results are also shown for completeness. These results are less accurate in the reproduction of the FDSM calculations. Nevertheless, the F-spin purity is also confirmed.

TABLE VI. Energies in MeV and maximal F-spin content of some low-lying states of ^{134}Ba calculated in the FDSM using Dyson boson mapping (first two columns), BZ mapping of the FDSM (second two columns), and seniority mapping A of the FDSM (the last two columns). The parameters of the Hamiltonian are taken from Ref. [7]. For details see the text.

	FDSM		BZ		sen A	
	Energy	max F spin	Energy	max F spin	Energy	max F spin
0_1^+	0.0000	0.93	0.0000	0.93	0.0000	0.97
0_2^+	1.7201	0.99	1.7284	0.99	1.7937	0.99
0_3^+	1.7938	0.77	1.8471	0.77	2.0234	0.79
0_4^+	2.5380	0.09	2.5561	0.09	2.4820	0.03
2_1^+	0.5559	0.95	0.5563	0.95	0.6069	0.99
2_2^+	1.1362	0.97	1.1401	0.97	1.2174	0.98
2_3^+	1.9619	0.08	1.9759	0.07	1.9398	0.03
2_4^+	2.5176	0.08	2.5292	0.08	2.4692	0.03
3_1^+	1.8857	0.98	1.8943	0.98	1.9596	0.99
4_1^+	1.3303	0.97	1.3350	0.97	1.4102	0.98
4_2^+	1.9998	0.98	2.0085	0.98	2.0741	0.99
4_3^+	2.5288	0.06	2.5400	0.06	2.4689	0.02
5_1^+	2.8823	0.97	2.8941	0.97	2.8903	0.97
6_1^+	2.3136	0.96	2.3228	0.97	2.3869	0.97
6_2^+	3.0621	0.98	3.0739	0.98	3.0706	0.97

One may ask whether the above observed feature of F-spin purity of the FDSM mapped states is an inherent property of the model or just a consequence of the particular SO$^\pi$(8)×SO$^\nu$(8) model case. For a comparison, maximal F-spin content from ^{196}Pt calculations in the SO$^\pi$(8)×Sp$^\nu$(6) limit is given in Table III. In the latter case, the F spin is not a good quantum number at all. This is rather transparent in terms of the boson mapping analysis. In the SO$^\pi$(8)×SO$^\nu$(8) calculations, the differences in the quadrupole-quadrupole strengths between like and unlike nucleons are responsible for the F-spin breaking ($\Delta\kappa$ breaking). In the SO$^\pi$(8)×Sp$^\nu$ (6) limit, the different ratios of the d-boson-conserving to the d-boson-changing parts in the proton and neutron quadrupole operators also cause the F-spin mixing ($\Delta\chi$ breaking). It is indeed known that the effect of $\Delta\chi$ breaking is much more important for F-spin impurity than that coming from $\Delta\kappa$ breaking [34].

Note that in the boson Hamiltonian mapped from the FDSM one, no Majorana interaction is present (the BZ calculations are completely equivalent to IBM-2). The

mechanism of splitting between normal and exotic states due to the proton-neutron quadrupole-quadrupole interaction is also effective in the IBM-2. In fact, this was observed earlier in some analyses [35].

Finally, one should inspect whether the p-n $Q\cdot Q$ splitting mechanism could solely explain the observed nuclear features. For the ^{134}Ba nucleus, this is indeed the case. For ^{196}Pt, however, the above calculated F-spin mixing is larger than that obtained from phenomenological analysis [36]. Here one would probably need some Majorana term in the IBM-2 to restore the F-spin breaking. Also the excitation energies of 2.1 MeV and 2.6 MeV for the mixed symmetry 1_1^+ state found from sample calculations for deformed nuclei in Sec. III A and from calculations for ^{148}Sm in Sec. III C, respectively, seem to be lower than the experimental values [37].

VI. DISCUSSION

For several examples, we have shown that for a given FDSM Hamiltonian one can construct from boson mappings an IBM-type boson Hamiltonian which yields similar results. The Dyson mapping reproduces the FDSM results exactly. This mapping is nonunitary and leads to non-Hermitian boson operators which somewhat obscures the relation between the FDSM and the phenomenological boson description. The unitary mappings, truncated to two-body terms in the boson Hamiltonian, approximate the exact results quite satisfactorily. Among these mappings the BZ mapping showed more universal applicability.

Note, however, that no degrees of freedom have been truncated in the boson space. In situations where, e.g., practical considerations force one to resort to this kind of truncation, the nontransformed Dyson and BZ mappings may not be reliable as the truncated space can represent a large component of the low-lying states in the mapped boson space. Here the seniority mapping approach often seems to be better equipped to capture the essence of a collective subspace [22,32].

We conclude that, apart from some differences clearly pointed out, a relation between the FDSM Hamiltonian and operators and those of the IBM-2 type have been satisfactorily demonstrated.

This does not, however, cover all aspects of the relation between the FDSM and IBM models. There remain different counting rules for the number of active normal parity fermion pairs in the FDSM and the number of valence-shell bosons in the IBM. When these differences are not too large, one might change the number of bosons in the IBM from N to $\tilde{N}$, while not varying the results drastically. In the IBM this may, e.g., be accommodated by modifying operators according to the substitution [38]

$$s^\dagger \to \sqrt{\frac{N-n_d}{\tilde{N}-n_d}}\,s^\dagger \approx \sqrt{\frac{\langle n_s\rangle}{N-\tilde{N}-\langle n_s\rangle}}\,s^\dagger , \qquad (6.1)$$

where $\langle n_s\rangle$ can be calculated as in Sec. II B. We thus deduce that for a particular FDSM description of a given nucleus, one can find a very similar explanation within the phenomenological IBM context. Of course, an account of a chain of nuclei in the FDSM with a constant set of parameters might require a varying parameter in the IBM. This is not unexpected in view of the natural N dependence of parameters which emerges in boson mappings.

A backward relation between the models is much less straightforward. The phenomenological IBM seems to offer wider possibilities and flexibility than the FDSM. For example, as follows from the FDSM to IBM mapping procedure, the quadrupole boson operators are restricted to be close to the O(6) or SU(3) limits for the SO(8) or Sp(6) fermion algebras, respectively. Analysis of real data might require departures from those IBM limits. An equivalent description within the FDSM could then only be achieved by including a two-body term of the type $(D^\dagger\tilde{D})^2$ in the fermion quadrupole operator [15]. Such a term maps in the lowest order onto $(D^\dagger\tilde{D})^2 \to (d^\dagger\tilde{d})^2$ and allows a greater flexibility in the mapped boson operator. Similarly, as discussion in Sec. V suggests, the Majorana term in the IBM might be needed in some cases for a correct description of the F-spin mixing and mixed symmetry states. In the lowest order, this term could be mapped from a four-body term in the FDSM Hamiltonian.

It seems appropriate at this stage to comment on a point of view often expressed about the relationship between the FDSM and IBM, namely, that the IBM derives from the FDSM when the Pauli principle is systematically neglected or, equivalently, that the IBM represents the $\Omega \to \infty$ limit of the FDSM [2]. This interpretation usually follows from a comparison of transition matrix elements based on a one-to-one correspondence between basis states and a simultaneously assumed simple correspondence between operators [2,8]. From the discussion in Sec. II we conclude that this is too restrictive an interpretation. When properly mapped operators are Hermitized and approximated to have coefficients depending on Ω and N only (no n_s or n_d dependence), then for fixed N the Pauli principle is clearly incorporated within an IBM framework, albeit in an approximate way. The crucial way in which Pauli principle differences will show up is in connection with spurious states (or allowed representations), as already discussed.

Apart from the previous paragraph, the discussion in this section pertains to the situation with only physical states in the mapped boson space. In those regions where spurious states appear, the FDSM and IBM descriptions differ essentially. It is thus imperative to look further into this aspect especially and FDSM analyses of the spectra of the relevant nuclei are really called for.

ACKNOWLEDGMENTS

This work has been supported by the Grant Agency of the Czech Republic under Grant No. 202/93/2472 and by grants from the South African Foundation for Research Development and the University of Stellenbosch.

[1] A. Arima and F. Iachello, *The Interacting Boson Model* (Cambridge University Press, Cambridge, England, 1987).
[2] C.-L. Wu, D.H. Feng, and M. Guidry, Adv. Nucl. Phys. (to be published).
[3] J.N. Ginocchio, Ann. Phys. (N.Y.) **126**, 234 (1980).
[4] A. Arima, N. Yoshida, and J.N. Ginocchio, Phys. Lett. B **101**, 209 (1981).
[5] C.-T. Li, V.G. Pedrocchi, and T. Tamura, Phys. Rev. C **33**, 1762 (1986).
[6] D.H. Feng, M.W. Guidry, X.-W. Pan, C.-L. Wu, and I. Zlatev, Phys. Rev. C**48**, R1488 (1993).
[7] X.-W. Pan and D.H. Feng, report, 1993.
[8] J.-Q. Chen, D.H. Feng, and C.-L. Wu, Phys. Rev. C **34**, 2269 (1986).
[9] M. Vallieres and H. Wu, in *Computational Nuclear Physics 1*, edited by K. Langanke *et al.* (Springer-Verlag, New York, 1991), p. 1.
[10] H.B. Geyer and F.J.W. Hahne, Nucl. Phys. **A363**, 45 (1981).
[11] E.A. de Kock and H.B. Geyer, Phys. Rev. C **42**, 1177 (1991).
[12] H.B. Geyer, C.A. Engelbrecht, and F.J.W. Hahne, Phys. Rev. C **33**, 1041 (1986).
[13] J. Dobaczewski, H.B. Geyer, and F.J.W. Hahne, Phys. Rev. C **44**, 1030 (1991).
[14] O. Scholten, in *Computational Nuclear Physics 1*, edited by K. Langanke *et al.* (Springer-Verlag, New York, 1991), p. 88.
[15] A. Arima, J.N. Ginocchio, and N. Yoshida, Nucl. Phys. **A384**, 112 (1982).
[16] P. Navrátil, H.B. Geyer, J. Dobeš, and J. Dobaczewski, Ann. Phys. (N.Y.) (submitted).
[17] J. Joubert and F.J.W. Hahne, S. Afr. J. Phys. **11**, 51 (1988).
[18] J. Joubert, F.J.W. Hahne, P. Navrátil, and H.B. Geyer, Phys. Rev. C (submitted).
[19] H.B. Geyer, Phys. Rev. C **34**, 2373 (1986).
[20] E.A. de Kock and H.B. Geyer, Phys. Rev. C **38**, 2887 (1988).
[21] P. Navrátil and J. Dobeš, Nucl. Phys. **A507**, 340 (1990).
[22] P. Navrátil and J. Dobeš, Phys. Rev. C **40**, 2371 (1989).
[23] T. Tamura, Phys. Rev. C **28**, 2480 (1983); T. Takada, *ibid.* **34**, 750 (1986).
[24] T. Otsuka, A. Arima, and F. Iachello, Nucl. Phys. **A309**, 1 (1978).
[25] T. Otsuka, A. Arima, F. Iachello, and I. Talmi, Phys. Lett. **B76**, 139 (1978).
[26] D. Bonatsos and A. Klein, Phys. Rev. C **31**, 992 (1985).
[27] H.G. Börner, J. Jolie, S. Robinson, R.F. Casten, and J.A. Cizewski, Phys. Rev. C **42**, R2271 (1990).
[28] A. Mauthofer, K. Stelzer, J. Idzko, Th.W. Elze, H.J. Wollersheim, H. Emling, P. Fuchs, E. Grosse, and D. Schwalm, Z. Phys. A **336**, 263 (1990).
[29] P. Navrátil and J. Dobeš, Nucl. Phys. **A533**, 223 (1991).
[30] R.F. Casten and J.A. Cizewski, Phys. Lett. B **185**, 293 (1987).
[31] P. Navrátil and H.B. Geyer, Nucl. Phys. **A556**, 165 (1993).
[32] P. Navrátil and J. Dobeš, Phys. Rev. C **46**, 220 (1992).
[33] A. Arima, T. Otsuka, F. Iachello, and I. Talmi, Phys. Lett. **B66**, 205 (1977).
[34] A.E.L. Dieperink, O. Scholten, and D.D. Warner, Nucl. Phys. **A469**, 173 (1987); P. Van Isacker, P.O. Lipas, K. Helimäki, I. Koivistoinen, and D.D. Warner, *ibid.* **A476**, 301 (1988); J. Dobeš, Phys. Lett. B **219**, 389 (1989).
[35] T. Otsuka and J.N. Ginnochio, Phys. Rev. Lett. **54**, 777 (1985); J. Dobeš, Nucl. Phys. **A469**, 424 (1987).
[36] A. Wolf, O. Scholten, and R.F. Casten, Phys. Lett. B **312**, 372 (1993).
[37] H.H. Pitz, U.E.P. Berg, R.D. Heil, U. Kneissl, R. Stock, C. Wesselborg, and P. von Brentano, Nucl. Phys. **A492**, 411 (1989); W. Ziegler, C. Rangacharyulu, A. Richter, and C. Spieler, Phys. Rev. Lett. **65**, 2515 (1990).
[38] V. Paar, in *Interacting Bosons in Nuclear Physics*, edited by F. Iachello (Plenum Press, New York, 1979), p. 163.